Low-Loss Silicon Strip-to-Slot Mode Converters

R. Palmer,[1,2] L. Alloatti,[1] D. Korn,[1] W. Heni,[1] P. C. Schindler,[1] J. Bolten,[3] M. Karl,[3] M. Waldow,[3] T. Wahlbrink,[3] W. Freude,[1,2] C. Koos,[1,2] and J. Leuthold[1,2]

[1]Institute of Photonics and Quantum Electronics (IPQ), Karlsruhe Institute of Technology (KIT), 76131 Karlsruhe, Germany
[2]Institute of Microstructure Technology (IMT), Karlsruhe Institute of Technology (KIT), 76344 Eggenstein-Leopoldshafen, Germany
[3]AMO GmbH, 52074 Aachen, Germany

DOI: 10.1109/JPHOT.2013.2239283
1943-0655/$31.00 ©2013 IEEE

Manuscript received November 21, 2012; revised December 17, 2012; accepted December 17, 2012. Date of publication January 15, 2013; date of current version February 5, 2013. This work was supported in part by the DFG Center for Functional Nanostructures, by the KIT Initiative of Excellence, by the Karlsruhe School of Optics and Photonics, by the EU-FP7 projects EURO-FOS under Grant 224402, SOFI under Grant 248609, and PHOXTROT, by the BMBF joint project MISTRAL funded by the German Ministry of Education and Research under Grant 01BL0804, and by the European Research Council (ERC Starting Grant "EnTeraPIC," number 280145). Corresponding author: R. Palmer (e-mail: robert.palmer@kit.edu).

Abstract: We demonstrate compact highly efficient broadband strip-to-slot mode converters in silicon with record-low losses of 0.02 (±0.02) dB and negligible reflections between 1480 nm and 1580 nm. The new strip-to-slot transition is logarithmically tapered, which enables a compact design. The new logarithmic tapers are compared with more conventional linearly tapered converters.

Index Terms: Photonic integrated circuits, optical waveguides.

1. Introduction

Strip-to-slot mode converters are key elements for linking well-established strongly guiding strip waveguides to slot waveguides that attracted recent interest for building active silicon devices.

Slot waveguides [1], [2] offer new possibilities to functionalize silicon waveguides by hybridization of silicon with highly nonlinear organic materials. While the fundamental material properties of silicon prohibit lasing and Pockels-effect-based modulation, organic materials can be engineered to complement missing properties of silicon such as optical gain [3], [4] and second-order nonlinearity [5]–[9]. The silicon-organic hybrid (SOH) approach [2], where strongly guiding silicon waveguides are covered with an organic cladding, combines the advantages of both materials. To efficiently exploit the nonlinear properties of the organic cladding, the interaction between guided field and cladding needs to be maximized. Therefore, slot waveguides formed by two silicon "rails" with a gap in between [see Fig. 1(b)] have been found to be superior to more conventional strip waveguides [see Fig. 1(a)]. Using slot waveguides covered with a nonlinear organic cladding, high-data rate all-optical signal processing has been demonstrated [10], [11]. Also, energy-efficient liquid crystal phase shifters [12] and high-speed modulation exploiting the ultrafast Pockels effect [5]–[8] take advantage of slightly modified so-called "striploaded" slot waveguides [see Fig. 1(c)]. These n-doped strips adjacent to the rails provide an electrical connection to RF transmission lines,

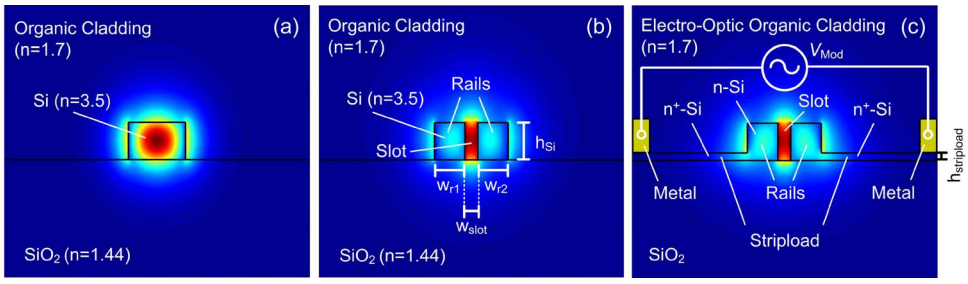

Fig. 1. Different types of silicon waveguides. (a) Strip waveguide with dimensions of 220 nm $\times$ 450 nm. The light is strongly confined in the silicon strip. (b) Slot waveguide with a rail width of $w_{r1,2} = 240$ nm each and a slot width of $w_{slot} = 100$ nm. The light is strongly confined in the slot. This allows to efficiently exploit the optical properties of an organic cladding material. (c) Strip-loaded slot waveguide of same dimensions as in (b). Metal electrodes are connected to the two rails of the slot waveguide by doped 45 nm high silicon strips (striplod). The slot is filled with an organic electro-optic material. An applied alternating voltage (V_{Mod}) drops essentially across the slot. The resulting strong electric field effectively changes the refractive index, thus enabling modulators with low V_π voltage.

which control a strong electric field inside the 100 nm-wide slot filled with the organic cladding. The strips act as an RF "load" for the slot waveguide capacitance.

However, most of the components realized in silicon photonics are based on strip waveguides that have low propagation loss of 2 dB/cm, even for small bend radii [13], while slot waveguide losses are usually in the order of (7–20) dB/cm [14]. Therefore, an efficient strip-to-slot waveguide transition is needed to exploit the advantages of each waveguide type. Efficient strip-to-slot mode converters are therefore key components. Dependent on the application the goal is to couple strip waveguides [see Fig. 1(a)] to slot waveguides [see Fig. 1(b)] or strip waveguides to striploaded slot waveguides [see Fig. 1(c)]. Such a converter between the waveguide types needs to have low losses, as well as low reflection to avoid multipath interference. If a strip waveguide should be coupled to a striploaded slot waveguide, in addition, the two rails of the slot waveguide need to be electrically insulated as each of the slot waveguide rails is in electrical contact with an electrode having a different potential [8]. Previously proposed strip-to-slot converters were based on linear tapers [15], [5]. A Y-shaped converter has been proposed by Brosi *et al.* [5], and a loss of 0.13 dB has been reported meanwhile for a 9 μm-long converter [16]. The fabrication of such a converter however is challenging for optical lithography, since it requires sub-100 nm features. Recently, a short strip-to-striploaded slot converter, which is more suitable for photolithography, has been demonstrated based on a spline taper with a loss of 0.8 dB for a 5 μm-long converter [17].

We experimentally demonstrate, to the best of our knowledge, the first strip-to-slot mode converters with less than 0.05 dB insertion loss, 0.02 dB in the best case, for converters with length of 7.5 μm and 16 μm, respectively. The average loss of the shortest fabricated converter of 4.5 μm length was only 0.26 dB per converter. The converters are based on a sophisticated design consisting of three taper sections that are independently optimized. Logarithmic tapers are used to reduce the length of the converters. The design avoids sub-100 nm features making the design compatible to 193 nm deep UV lithography. The design combines all the advantages of ease of fabrication, electrical insulation in combination with ultra-low reflections, and short length. We believe it is a key component for versatile SOH devices combining the advantages of high-index contrast waveguides and specially engineered organics.

2. Mode Converter Design

For converting one modal field into a different one, adiabatic transitions are desired. For strip-to-slot transitions, logarithmically tapered waveguide transitions have been found to have lower conversion losses and reduced length as compared to linear transitions, as will be shown in Section 3.2.

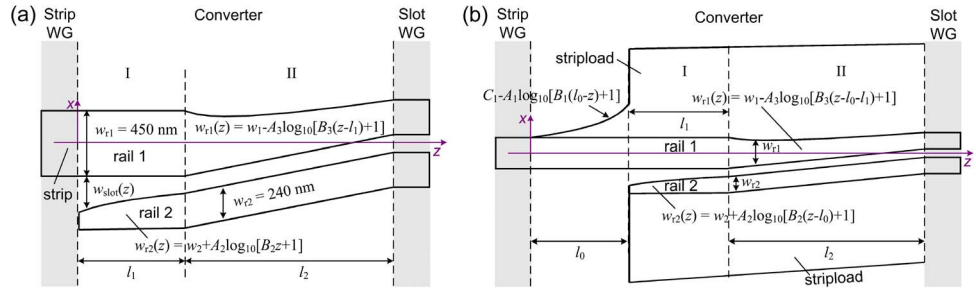

Fig. 2. Schematic of the converter based on logarithmic tapers. (a) Strip-to-slot converter. The converter is split in two sections. In Section 1 the width of rail 2 is logarithmically uptapered from 120 nm to 240 nm. Conversely, the width of the slot is simultaneously downtapered from 240 nm to 120 nm. In Section 2 the slot width w_{slot} and the width w_{r2} of rail 2 remain constant, while the width w_{r1} of rail 1 is tapered down from 450 nm to 240 nm. (b) Schematic of a converter between a strip waveguide and a striploaded slot waveguide. Here, to the left of Section 1, the silicon stripload is uptapered. Parameters: $A_1 = 500$ nm, $A_2 = 200$ nm, $A_3 = 200$ nm, $B_1 = 2.25\ \mu\text{m}^{-1}$, $B_2 = 0.87\ \mu\text{m}^{-1}$, $B_3 = 1.28\ \mu\text{m}^{-1}$, $C_1 = 525$ nm, $w_1 = 450$ nm, $w_2 = 120$ nm, $l_0 = 4\ \mu$m.

Fig. 2 depicts two schemes of mode converters. Fig. 2(a) shows a converter for coupling a strip waveguide [see Fig. 1(a)] to a slot waveguide [see Fig. 1(b)]. The width of the two rails of the slot waveguide is logarithmically tapered in separate sections. Fig. 2(b) shows a converter between strip waveguide [see Fig. 1(a)] and strip-loaded slot waveguide [see Fig. 1(c)] as needed for SOH modulators [8], [2]. The two rails of the slot waveguide are connected to 45 nm high silicon strips (stripload) in this case. A third taper section is added prior to Section 1 to asymmetrically add a stripload to rail 1. An SOH modulator requires that the two rails of the slot waveguide are electrically insulated, since they are connected to electrodes of different potential. The converter fulfills this requirement and combines it with low insertion loss and low reflections.

3. Simulation

In this section, the transmission properties of the converter are studied. The choice of the logarithmic shape of the converters is justified, and the logarithmically tapered strip-to-slot converters are compared to linearly tapered converters. In addition, the influence of slot waveguide parameters is investigated.

3.1. Proper Choice of the Taper Shape

Decades before scientists studied the first adiabatic mode transitions of planar optical waveguides, the problem of mode conversion was studied intensively by the electrical engineering community in the context of antennas or striplines. The intention was usually to transform one wave impedance of a metallic waveguide into another impedance while simultaneously keeping reflections low. The reflections at the input of such an inhomogeneous metallic waveguide were calculated by approximating the taper with a sequence of short sections of constant impedance and by summing over all partial reflections [18]. To achieve a short transition with low reflections, a variety of taper shapes like parabolic, exponential, hyperbolic cosine, and triangular have been proposed.

The choice of the proper impedance taper function depends on the application in terms of length, allowed reflection, and bandwidth, e.g., the exponential taper is among the shortest if a moderate reflection factor is not crucial, while a slightly longer so-called “triangular” [18, Eq. (5.71)] taper results in much lower reflections. For long transitions, linear and nonlinear taper functions perform equally well.

Though the same taper functions are often used for dielectric waveguide tapers, the optimization criterion is slightly more restricted. The guided power should be conserved; thus, not only reflection but also radiation of power should be avoided. An approach to solve this problem was introduced by Milton and Burns [19]. They derived the optimum taper geometry for a transition from a 2 μm wide

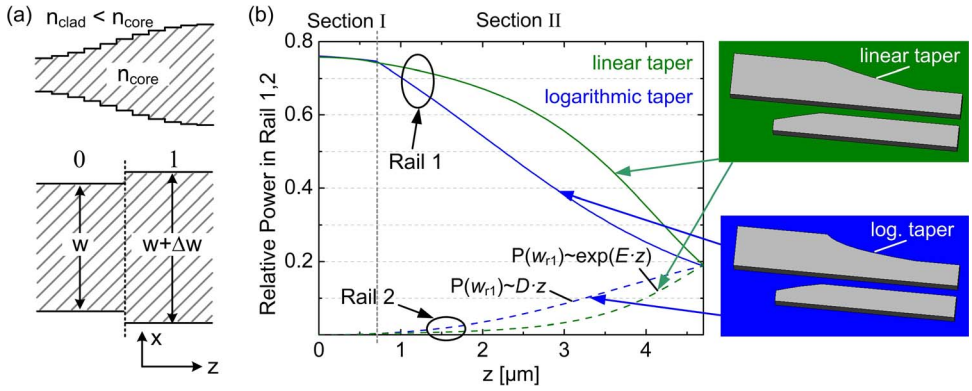

Fig. 3. (a) Approximation of a taper by a series of small steps. The width of the structure is only slightly changing from segment to segment. In order to have a nearly adiabatic transition the coupling coefficient between the neighboring segments needs to be close to unity. Modified after [19]. (b) Power guided in rail 1 and rail 2 normalized to the total cross-sectional power. Comparison between linear and logarithmic taper. The figure demonstrates that a logarithmic taper results in a near ideal compact close-to-adiabatic transmission. In the linear case the power guided in rail 2 increases exponentially. Applying the step transition model we therefore expect a steady decrease of the coupling coefficients. For the logarithmic taper the power in rail 2 increases nearly linearly. Therefore, we expect an almost constant coupling coefficient between the individual taper segments in the logarithmic case which corresponds to the shortest realization of an adiabatic transition.

planar waveguide to a 50 μm wide channel waveguide. The ansatz was to use the step transition model of Marcuse [20] [see Fig. 3(a)]. The locally transmitted power from hybrid mode i to mode j at each step of the taper can be calculated by an overlap integral between the modal electric and magnetic field vectors $\vec{E}_{(i,j)(0,1)}$, $\vec{H}_{(i,j)(0,1)}$ to the left (subscript 0) and to the right (subscript 1) of the transition in analogy to the working principle of mode expansion solvers [21]. The coupling coefficient between local mode i to the left of the transition and local mode j to the right of the transition is given by [19]

$$c_{ij} = \frac{\int_{-\infty}^{\infty}\int_{-\infty}^{\infty}\left[\left(\vec{E}_{i0}\times\vec{H}_{j1}^{*}\right)_z+\left(\vec{E}_{j1}^{*}\times\vec{H}_{i0}\right)_z\right]\mathrm{d}x\,\mathrm{d}y}{2\left[\int_{-\infty}^{\infty}\int_{-\infty}^{\infty}\left[\left(\vec{E}_{i0}\times\vec{H}_{i0}^{*}\right)_z\right]\mathrm{d}x\,\mathrm{d}y\int_{-\infty}^{\infty}\int_{-\infty}^{\infty}\left[\left(\vec{E}_{j1}\times\vec{H}_{j1}^{*}\right)_z\right]\mathrm{d}x\,\mathrm{d}y\right]^{1/2}}.$$

For a close to adiabatic transition, all modes to the left should couple to the equivalent modes to the right with a coupling coefficient close to one, while the cross couplings should be as small as possible. In mathematical terms, this means $c_{ij} \approx \delta_{ij}$, where δ_{ij} is the Kronecker symbol. Under the assumption that the effective width of the waveguide is equivalent to its physical width and restricting the design to small taper angles, the authors [19] find that the nearly ideal taper function is a parabola. However, for narrow strongly confining high index contrast waveguides, this assumption does not hold anymore since the evanescent field of the guided mode is in the order of the physical width of the waveguide. Nevertheless, for high index contrast structures, many other authors found exponential and parabolic tapers to work well [22], [23].

For the strip-to-slot converter under consideration, neither the parabolic taper nor the exponential taper can directly be used because of the following reasons: First, the effective width here is much different from the physical dimensions, and second, we consider a transition from a one-rail structure to a coupled two-rail waveguide. However, the criterion formulated by Milton and Burns [19] still holds: The most compact adiabatic transition between two modal field distributions is achieved when the coupling coefficient c_{ii} remains constant and close to unity along the taper length. Therefore, the requirement is that the difference in the modal field distributions of the two sides of each step should be small. In order to get the shortest possible solution, the differential change $dF(x, y, z)/dz$ of the modal field distribution $F(x, y, z)$ should be constant such that the coupling

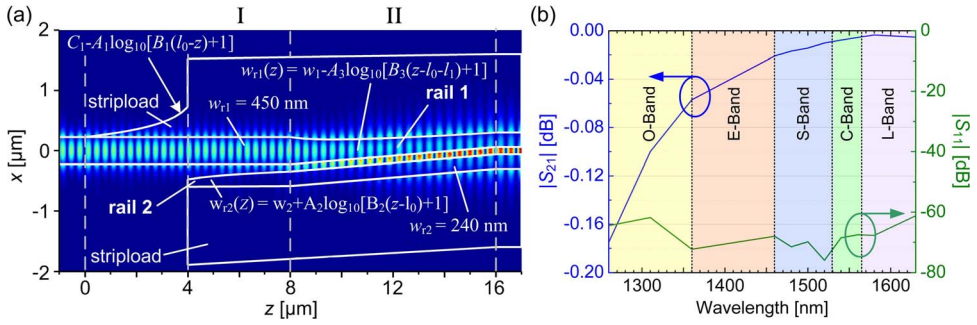

Fig. 4. (a) Electric field distribution in the logarithmically tapered strip-to-striploaded slot mode converter. To the left of Section 1 a one-sided logarithmic uptaper of the stripload is added. In Section 1 the slot width w_{slot} is logarithmically tapered down from 240 nm to 120 nm (rail 2 tapered up from 120 nm to 240 nm). Section 2 comprises the logarithmic taper of rail 1 to the final symmetric strip-loaded slot waveguide. The slot width and the width of rail 2 remain constant in this section. The simulated loss at 1550 nm is found to be 0.01 dB, while the reflection factor $|S_{11}|$ is below -60 dB. (b) Simulated S-parameters of the converter as a function of frequency. Transmission and reflection factor $|S_{21}|$ and $|S_{11}|$. The simulated losses are predicted to be below 0.2 dB (reflection factor below -60 dB) over a wide spectrum comprising the O, E, S, C, and L-band. Parameters: $A_1 = 500$ nm, $A_2 = 200$ nm, $A_3 = 200$ nm, $B_1 = 2.25\ \mu\text{m}^{-1}$, $B_2 = 0.87\ \mu\text{m}^{-1}$, $B_3 = 1.28\ \mu\text{m}^{-1}$, $C_1 = 525$ nm, $w_1 = 450$ nm, $w_2 = 120$ nm, $l_0 = 4\ \mu$m, $l_1 = 4\ \mu$m, $l_2 = 8\ \mu$m.

coefficient remains constant. Fig. 3(b) shows the power guided in rail 1 and rail 2 normalized to the total cross-sectional power while tapering down rail 1 for the case of a linear taper and a logarithmic taper.

The linear taper is an example for an unoptimized taper. It can be seen from Fig. 3(b) that the guided power couples exponentially to rail 2 if the width of rail 1 is linearly downtapered. Therefore, the coupling coefficient monotonically decreases along the taper. However, our goal is to achieve a constant differential change in the modal field distribution. This corresponds, to a first approximation, to a linear power exchange between the two rails as rail 1 is downtapered along z. Since the power transfer is found to be nearly exponential along a linear taper, a linear power transfer can be achieved by using the inverse function, namely, a logarithmic taper, as depicted in Fig. 3(b). It can be seen that, for the logarithmic taper, the power coupled to rail 2 increases nearly linearly. Therefore, we expect that the logarithmically tapered converter is close to ideal.

3.2. Linearly Tapered Converter versus Logarithmically Tapered Converter

Strip-to-slot mode converters based on linear and logarithmic tapers are investigated and compared. It will be shown that a logarithmic taper can outperform a linear taper for short transitions. The minimum length of the converter is mainly determined by taper Section 2 in Fig. 2.

The conversion between a strip and a strip-loaded slot waveguide is depicted in Fig. 4(a). The figure shows the distribution of the quasi-TE polarized electric field. The performance of the converter has been simulated by a finite integration method using the commercial simulation tool CST Microwave Studio. Our simulations predict losses in the order of 0.01 dB at 1550 nm. In a wavelength range from 1260 nm to 1675 nm (comprising the O-, E-, S-, C-, and L-Band), the simulation shows losses below 0.2 dB, and the reflection factor has been found to be below -60 dB.

The losses in the two sections of the converter are studied separately in Fig. 5(a) and (b). First, the length of Section 1 in Fig. 2 is varied while keeping all parameters of Section 2 constant, Fig. 5(a). The transmission $(|S|_{21})$ and reflection factor $(|S|_{11})$ are observed. It can be seen that the length of Section 1 has only little impact on the performance of the converter. Loss and reflection are small even for a taper length smaller than 1 μm. This section mainly helps keeping reflections low. The benefit of tapering logarithmically instead of linearly is minor for this section. In contrast, the length of Section 2 has a stronger impact on the transmission properties of the converter [see Fig. 5(b)]. A logarithmic taper outperforms the linear transition by up to 0.3 dB for short taper

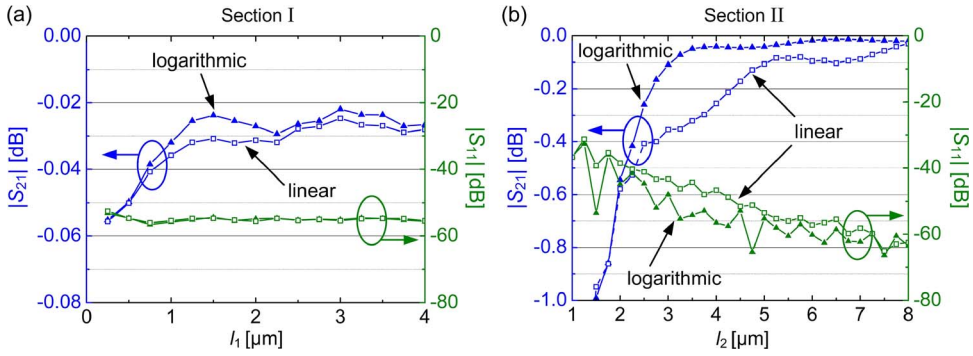

Fig. 5. (a) Comparison between linear and logarithmic taper in Section 1. The length of the taper is varied. In this simulation of Section 1 we chose a Section 2 with 4 μm long logarithmic taper. The transmission is high even for tapers as short as 700 nm. Using a logarithmic taper in Section 1 gives some small advantages. The reflection is nearly constant down to shortest lengths. (b) Comparison between linear and logarithmic taper in Section 2. The length of the taper is varied. For Section 1 a 700 nm long logarithmic taper has been chosen. For a taper length in Section 2 that is between 2 μm and 8 μm a logarithmic taper results in up to 0.3 dB lower losses as compared to a linear taper of same length. Above a length of 8 μm the linear and logarithmic taper perform alike. The reflection coefficient becomes smaller as the length of the taper is increased. The reflection is slightly lower for a logarithmic taper.

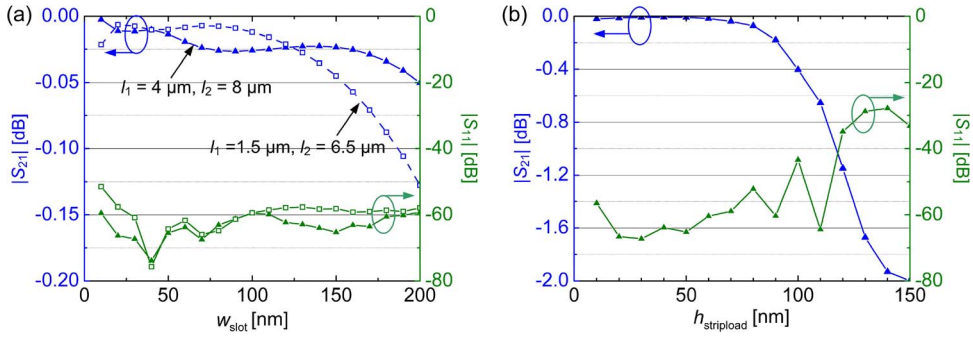

Fig. 6. Variation of waveguide parameters. (a) Transmission and reflection of a strip-to-slot converter for different slot sizes. Two converter lengths are investigated. The longer converter outperforms the shorter converter for slots wider than 130 nm. (b) The impact of the striploaded height on the performance of the converter is investigated. The converter loss is below 0.2 dB up to a striploaded height of 90 nm. This makes the converter robust against fabrication tolerances.

lengths from 2 μm up to 8 μm. For longer tapers, linear and logarithmic tapers perform alike as expected.

3.3. Impact of Slot Waveguide Parameters on Converter Performance

The impact of the slot waveguide parameters on the converter performance is studied. First, the slot width of the logarithmic strip-to-slot converter is varied while keeping the width of the rails constant [see Fig. 6(a)]. 12 μm ($l_1 + l_2 = 4\ \mu\text{m} + 8\ \mu\text{m}$) and 8 μm ($l_1 + l_2 = 1.5\ \mu\text{m} + 6.5\ \mu\text{m}$) long strip-to-slot converters are investigated. Since coupling between the two rails becomes weaker for bigger slots, a better performance is achieved by the longer converter for a slot width bigger than 130 nm. Fig. 6(b) shows the influence of the height of the striploaded on the transmission properties of the strip-to-striploaded slot mode converter. Its total length is 16 μm ($l_0 + l_1 + l_2 = 4\ \mu\text{m} + 4\ \mu\text{m} + 8\ \mu\text{m}$). The converter loss is below 0.2 dB up to a striploaded height of 90 nm.

In conclusion, the converter is only weakly affected by a change of the slot width or striploaded height. This makes the converter robust against fabrication tolerances.

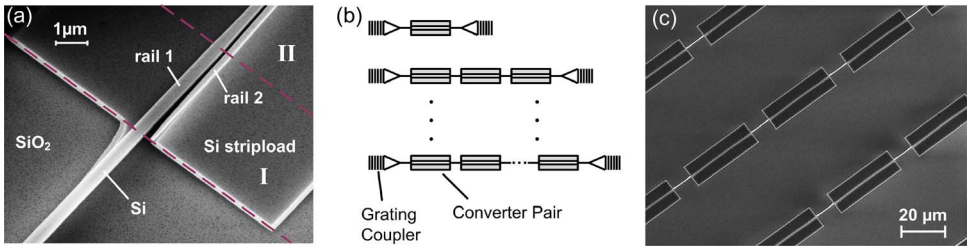

Fig. 7. (a) SEM image of a fabricated strip-to-striploaded slot mode converter. (b) Schematic of the chip layout for "cut-back" measurements. Pairs of converters (from strip-to-slot and back) are arranged in series. The number of converter pairs is varied. Light is coupled to the converters by using grating couplers, as reported in [24]. (c) SEM image of the "cut-back" structures.

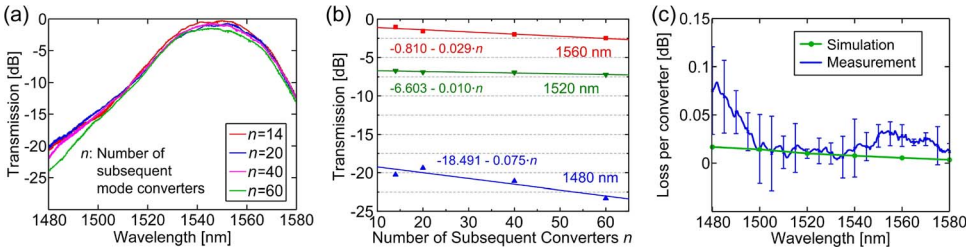

Fig. 8. (a) Normalized transmission spectra of series of 14, 20, 40, and 60 equally spaced mode converters (pairs of 7, 10, 20, and 30 converters). The spectra do not show any ripples which indicates that there are few if any reflections. The frequency dependency of the spectra is a property of the grating couplers alone [14]. (b) Linear regression of transmission in dB versus number of converters for three exemplary wavelengths. From the slope of the regression the loss per converter at this wavelength can be inferred. (c) Loss per converter as a function of wavelength. The loss is below 0.1 dB in the entire measured spectral range. The error bars indicate the 68% $(\pm\sigma)$ confidence interval. The measurement accuracy was mainly limited by fabrication non-uniformities of the grating couplers. Dimensions: $l_0 = 4\ \mu$m, $l_1 = 4\ \mu$m, $l_2 = 8\ \mu$m.

4. Fabrication and Characterization

Logarithmically tapered converters between strip and strip-loaded slot waveguides were fabricated on an SOI wafer with a 220 nm silicon device layer and 3 μm thick buried oxide. Converter prototypes were fabricated in the cleanroom facilities of AMO GmbH employing AMO's integrated silicon nanophotonic platform. Definition of the photonic devices has been carried out by electron beam lithography (EBL) using hydrogen silsesquioxane (HSQ) as a negative tone resist material. Using HSQ and advanced proximity correction procedure allowed for a precise control of lateral dimensions of the fabricated converters. Pattern transfer into the silicon has been carried out by using a reactive ion etching process based on HBr chemistry. Special care was taken to achieve a high degree of anisotropy and a low sidewall roughness. In total, two consecutive process modules, consisting of EBL and HBr-based etching, have been employed for realizing the two different etch depths of the slot waveguide with 45 nm high silicon striploads. Although EBL-based fabrication for fast prototyping has been used, the design can, in principle, be realized by using 193 nm deep UV lithography as it does not comprise sub-100 nm features. An SEM image of a fabricated mode converter is depicted in Fig. 7(a). The devices were covered with an 800 nm thick layer of PMMA (950k). We characterized several mode converter pairs in series [see Fig. 7(b) and (c)]. The number of subsequent converter pairs was varied. This allows extracting the loss per converter similar to a cut-back measurement. Light was coupled to the chip using grating couplers, identical to the ones reported in [24]. Access waveguides had a constant length. In that way, the extracted loss per converter was not affected by the access waveguides. The measured loss therefore comprises the transition loss and the propagation loss of the converter.

TABLE 1

Measured loss of the fabricated mode converters averaged in the wavelength range between 1480 nm and 1580 nm. The error bars indicate the 68% $(\pm\sigma)$ confidence intervals. Dimensions: $l_0 = 4$ μm, $l_1 = 4$ μm, $l_2 = 8$ μm

Sample	1	2	3
Average Insertion Loss per Converter [dB]	0.05 ± 0.06	0.04 ± 0.02	0.02 ± 0.02

TABLE 2

Measured loss of mode converters of different length averaged in the wavelength range between 1480 nm and 1580 nm. The error bars indicate the 68% $(\pm\sigma)$ confidence intervals

Total length [µm]	**4.5**	**7.5**	**16**
Length of stripload taper [µm]	1.5	1.5	4
Length of section I [µm]	0.5	1.5	4
Length of section II [µm]	2.5	4.5	8
Average Insertion Loss per Converter [dB] – Sample 4	0.18 ± 0.06	0.05 ± 0.02	0.03 ± 0.04
Average Insertion Loss per Converter [dB] – Sample 5	0.34 ± 0.06	0.05 ± 0.04	0.03 ± 0.03
Simulated Loss per Converter [dB]	**0.21**	**0.05**	**0.01**

A first set of three nominally identical samples has been fabricated. A tunable laser source and an optical spectrum analyzer were used to measure the transmission spectrum of the devices in a wavelength range between 1480 nm and 1580 nm. As can be seen in Fig. 8(a), the spectra of the series connected mode converters do not exhibit superimposed oscillations, even in the case of 60 converters in series, underlining that the reflection coefficient of the converter is indeed very low. The frequency dependence of the spectra stems from the grating couplers and is not a property of the converters. The loss per mode converter, depicted in Fig. 8(c), was extracted by a linear regression of total loss versus number of converters at each wavelength separately [see Fig. 8(b)]. The error bars represent the 68% $(\pm\sigma)$ confidence intervals. The measured loss agrees well with the simulations. Table 1 summarizes the measurement results of three identical chips, averaged over the measured spectral range (1480 nm to 1580 nm). The measured losses were reproducible and well below 0.1 dB, in the best case 0.02 dB per converter. The measurement accuracy was mainly limited by fabrication nonuniformities of the grating couplers. This is, to the best of our knowledge, the lowest reported loss for a mode converter between a strip waveguide and a striploaded slot waveguide.

A fourth and a fifth sample (samples 4 and 5) were fabricated comprising converters of different lengths. Table 2 shows the measured losses of the converters, as well as the expected simulated loss. The shortest converter was 4.5 μm in length and had a loss of 0.18 dB, in the best case, 0.63 dB less than the best previously reported strip-to-striploaded slot converters [17] and slightly shorter. Converters with 7.5 μm and 16 μm length had similar insertion loss of only 0.05 dB and 0.03 dB, respectively, which agrees well with the simulated data in Fig. 5(c). The measured converter losses are in agreement with the simulation results.

5. Conclusion

We have demonstrated strip-to-striploaded slot converters with the so far lowest reported losses of (0.02 ± 0.02) dB in the C-band and beyond. The measured spectra prove that the optical reflection coefficient is negligible. In addition, the proposed mode converter keeps the rails of the slot waveguide electrically insulated, making it particularly suited for active SOH devices [3], [5].

Acknowledgment

We acknowledge technological support by the Karlsruhe Nano-Micro Facility (KNMF), by the Light Technology Institute (KIT-LTI) and the ePIXfab (silicon photonics platform). We are grateful to Prof. D. Gerthsen (KIT-LEM) for support in nano-inspection and analysis. We acknowledge support by Deutsche Forschungsgemeinschaft and Open Access Publishing Fund of Karlsruhe Institute of Technology.

References

[1] V. R. Almeida, Q. F. Xu, C. A. Barrios, and M. Lipson, "Guiding and confining light in void nanostructure," *Opt. Lett.*, vol. 29, no. 11, pp. 1209–1211, Jun. 1, 2004.
[2] J. Leuthold, W. Freude, J.-M. Brosi, R. Baets, P. Dumon, I. Biaggio, M. L. Scimeca, F. Diederich, B. Frank, and C. Koos, "Silicon organic hybrid technology—A platform for practical nonlinear optics," *Proc. IEEE*, vol. 97, no. 7, pp. 1304–1316, Jul. 2009.
[3] A. E. Vasdekis, S. A. Moore, A. Ruseckas, T. F. Krauss, I. D. W. Samuel, and G. A. Turnbull, "Silicon based organic semiconductor laser," *Appl. Phys. Lett.*, vol. 91, no. 5, pp. 051124-1–051124-3, Jul. 30, 2007.
[4] D. Korn, M. Lauermann, P. Appel, L. Alloatti, R. Palmer, W. Freude, J. Leuthold, and C. Koos, "First silicon-organic hybrid laser at telecommunication wavelength," in *Proc. CLEO*, 2012, pp. 1–2.
[5] J.-M. Brosi, C. Koos, L.C. Andreani, M. Waldow, J. Leuthold, and W. Freude, "High-speed low-voltage electro-optic modulator with a polymer-infiltrated silicon photonic crystal waveguide," *Opt. Exp.*, vol. 16, no. 6, pp. 4177–4191, Mar. 17, 2008.
[6] M. Hochberg, T. Baehr-Jones, G. Wang, J. Huang, P. Sullivan, L. Dalton, and A. Scherer, "Towards a millivolt optical modulator with nano-slot waveguides," *Opt. Exp.*, vol. 15, no. 13, pp. 8401–8410, Jun. 2007.
[7] J. H. Wuelbern, S. Prorok, J. Hampe, A. Petrov, M. Eich, J. Luo, A. K. Y. Jen, M. Jenett, and A. Jacob, "40 GHz electro-optic modulation in hybrid silicon-organic slotted photonic crystal waveguides," *Opt. Lett.*, vol. 35, no. 16, pp. 2753–2755, Aug. 15, 2010.
[8] L. Alloatti, D. Korn, R. Palmer, D. Hillerkuss, J. Li, A. Barklund, R. Dinu, J. Wieland, M. Fournier, J. Fedeli, H. Yu, W. Bogaerts, P. Dumon, R. Baets, C. Koos, W. Freude, and J. Leuthold, "42.7 Gbit/s electro-optic modulator in silicon technology," *Opt. Exp.*, vol. 19, no. 12, pp. 11 841–11 851, Jun. 6, 2011.
[9] L. Alloatti, D. Korn, C. Weimann, C. Koos, W. Freude, and J. Leuthold, "Second-order nonlinear silicon-organic hybrid waveguides," *Opt. Exp.*, vol. 20, no. 18, pp. 20 506–20 515, Aug. 2012.
[10] C. Koos, L. Jacome, C. Poulton, J. Leuthold, and W. Freude, "Nonlinear silicon-on-insulator waveguides for all-optical signal processing," *Opt. Exp.*, vol. 15, no. 10, pp. 5976–5990, May 14, 2007.
[11] C. Koos, P. Vorreau, T. Vallaitis, P. Dumon, W. Bogaerts, R. Baets, B. Esembeson, I. Biaggio, T. Michinobu, F. Diederich, W. Freude, and J. Leuthold, "All-optical high-speed signal processing with silicon-organic hybrid slot waveguidesx," *Nat. Photon.*, vol. 3, no. 4, pp. 216–219, Apr. 2009.
[12] J. Pfeifle, L. Alloatti, W. Freude, J. Leuthold, and C. Koos, "Silicon-organic hybrid phase shifter based on a slot waveguide with a liquid-crystal cladding," *Opt. Exp.*, vol. 20, no. 14, pp. 15 359–15 376, Jul. 2012.
[13] S. K. Selvaraja, W. Bogaerts, P. Absil, D. Van Thourhout, and R. Baets, "Record low-loss hybrid rib/wire waveguides for silicon photonic circuits," *Proc. 7th Int. Conf. Group IV Photon. (PD)*, 2010.
[14] T. Alasaarela, D. Korn, L. Alloatti, A. Säynätjoki, A. Tervonen, R. Palmer, J. Leuthold, W. Freude, and S. Honkanen, "Reduced propagation loss in silicon strip and slot waveguides coated by atomic layer deposition," *Opt. Exp.*, vol. 19, no. 12, pp. 11 529–11 538, Jun. 2011.
[15] J. Blasco and C. A. Barrios, "Compact slot-waveguide/channel-waveguide mode-converter," *Proc. CLEO/Eur.*, p. 607, 2005.
[16] Z. Wang, N. Zhu, Y. Tang, L. Wosinski, D. Dai, and S. He, "Ultracompact low-loss coupler between strip and slot waveguides," *Opt. Lett.*, vol. 34, no. 10, pp. 1498–1500, May 15, 2009.
[17] Y. Liu, T. Baehr-Jones, J. Li, A. Pomerene, and M. Hochberg, "Efficient strip to strip-loaded slot mode converter in silicon-on-insulator," *IEEE Photon. Technol. Lett.*, vol. 23, no. 20, pp. 1496–1498, Oct. 2011.
[18] D. M. Pozar, *Microwave Engineering*. New York: Wiley, 1998.
[19] A. Milton and W. Burns, "Mode coupling in optical waveguide horns," *IEEE J. Quantum Electron.*, vol. QE-13, no. 10, pp. 828–835, Oct. 1977.
[20] D. Marcuse, "Radiation loss of tapered dielectric slab wave guides," *Bell Syst. Tech. J.*, vol. 49, pp. 273–290, 1970.
[21] D. F. G. Gallagher and T. P. Felici, "Eigenmode expansion methods for simulation of optical propagation in photonics—Pros and cons," presented at the Proc. Photon. West, 2003.
[22] G. Ren, S. Chen, Y. Cheng, and Y. Zhai, "Study on inverse taper based mode transformer for low loss coupling between silicon wire waveguide and lensed fiber," *Opt. Commun.*, vol. 284, no. 19, pp. 4782–4788, Sep. 2011.
[23] V. R. Almeida, R. R. Panepucci, and M. Lipson, "Nanotaper for compact mode conversion," *Opt. Lett.*, vol. 28, no. 15, pp. 1302–1304, Aug. 2003.
[24] D. Taillaert, F. Van Laere, M. Ayre, W. Bogaerts, D. Van Thourhout, P. Bienstman, and R. Baets, "Grating couplers for coupling between optical fibers and nanophotonic waveguides," *Jpn. J. Appl. Phys.*, vol. 45, no. 8A, pp. 6071–6077, 2006.